The Astrophysical Journal Letters, 708:L42–L46, 2010 January 1 doi:10.1088/2041-8205/708/1/L42


# ON STRONG MASS SEGREGATION AROUND A MASSIVE BLACK HOLE: IMPLICATIONS FOR LOWER-FREQUENCY GRAVITATIONAL-WAVE ASTROPHYSICS

Miguel Preto[1] and Pau Amaro-Seoane[2,3]
[1] Astronomisches Rechen-Institut, Zentrum für Astronomie, University of Heidelberg, D-69120 Heidelberg, Germany
[2] Max Planck Institut für Gravitationsphysik (Albert-Einstein-Institut), D-14476 Potsdam, Germany
[3] Institut de Ciències de l'Espai (CSIC-IEEC), Campus UAB, Torre C-5, parells, 2na planta, ES-08193, Bellaterra, Barcelona, Spain
*Received 2009 October 18; accepted 2009 December 1; published 2009 December 16*

## ABSTRACT

We present, for the first time, a clear *N*-body (NB) realization of the *strong mass segregation* solution for the stellar distribution around a massive black hole (MBH). We compare our NB results with those obtained by solving the orbit-averaged Fokker–Planck (FP) equation in energy space. The NB segregation is slightly stronger than in the FP solution, but both confirm the *robustness* of the regime of strong segregation when the number fraction of heavy stars is a (realistically) small fraction of the total population. In view of recent observations revealing a dearth of giant stars in the sub-parsec region of the Milky Way, we show that the timescales associated with cusp re-growth are not longer than $(0.1-0.25)\times T_{rlx}(r_h)$. These timescales are shorter than a Hubble time for black holes masses $M_\bullet \lesssim 4\times10^6 M_\odot$ and we conclude that quasi-steady, mass-segregated, stellar cusps may be common around MBHs in this mass range. Since extreme mass ratio inspirals detection rates by *Laser Interferometer Space Antenna* are expected to peak for $M_\bullet \sim 4\times10^5$–$10^6\ M_\odot$, a good fraction of these events should originate from strongly segregated stellar cusps.

*Key words:* black hole physics – galaxies: nuclei – gravitational waves – stellar dynamics

## 1. INTRODUCTION

The distribution of stars around a massive black hole (henceforth MBH) is a classical problem in stellar dynamics (Bahcall & Wolf 1976; Lightman & Shapiro 1977). The observational demonstration of the existence of nuclear stellar clusters (henceforth NSCs)—as revealed by a clear upturn in central surface brightness—in the centers of galaxies makes its study ever more timely. A number of NSCs in coexistence with a central MBH have recently been detected (Graham & Spitler 2009) suggesting that NSCs around MBHs, like the one in the center of the Milky Way, may be quite common.

The renewed interest in this theoretical problem is thus motivated by the observational data in NSCs and, in particular, the very rich and detailed data available for the stars orbiting the Galactic MBH. At the same time, the prospects for detection of gravitational waves (GWs) from extreme mass ratio inspirals (henceforth EMRIs) with future GW detectors such as the *Laser Interferometer Space Antenna* (*LISA*) also urge us to build a solid theoretical understanding of sub-parsec structure of galactic nuclei. In fact, EMRI rates will depend strongly on the stellar density of compact remnants as well as on the detailed physics within $O(0.01\,\mathrm{pc})$ of the hole, which is the region from which these inspiralling sources are expected to originate (Hopman & Alexander 2005).

Bahcall & Wolf (1976) have shown, through a kinetic treatment, that, in the case where all stars are of the same mass, this quasi-steady distribution takes the form of power laws, $\rho(r)\sim r^{-\gamma}$, in physical space and $f(E)\sim E^p$ in energy space ($\gamma = 7/4$ and $p=\gamma-3/2=1/4$). This is the so-called *zero-flow solution* for which the net flux of stars in energy space is precisely zero. Preto et al. (2004) and Baumgardt et al. (2004a) were the first to report *N*-body (NB) realizations of this solution, thereby validating the assumptions inherent to the Fokker–Planck (FP) approximation—namely, that scattering is dominated by uncorrelated, two-body encounters and, in particular, dense stellar cusps populated with stars of the *same mass* are robust against the ejection of stars from the cusp.

The properties of stellar systems that display a range of stellar masses are only very poorly reproduced by single-mass models. It is well known from stellar dynamical theory that when several masses are present there is mass segregation—a process by which the heavy stars accumulate near the center while the lighter ones float outward (Spitzer 1987; Khalisi et al. 2007). Accordingly, stars with different masses get distributed with different density profiles. By assuming a stellar population with two mass components, Bahcall & Wolf (1977)—henceforth BW77—generalized their early cusp solution and argued heuristically for a scaling relation $p_L = m_L/m_H\times p_H$ that depends on the star's mass ratio only. However, they obtained no general result on the inner slope of the heavy objects; nor did they discuss the dependence of the result on the component's number fractions. On the other hand, it was shown long ago by Hénon (1969) that the presence of a mass spectrum leads to an increased rate of stellar ejections from the core of a globular cluster, but he did not include the presence of a MBH at the center. Hénon's work raises the question as to whether *multi-mass* stellar cusps, obtained from the solution of the FP equation, are robust against the ejection of stars from the cusp. Ejections—due to strong encounters—are a priori excluded from the FP evolution, even though they could occur in a real nucleus. Furthermore, even if cusps were shown by NB results to be robust against stellar ejections (and we show that they are in this Letter), BW77 scaling cannot be valid for arbitrary number fractions.

Recently, Alexander & Hopman (2009)—henceforth AH09—stressed this latter point and have shown via FP calculations that, indeed, in the limit where the number fraction of heavy stars is realistically small, a new solution that they coined, the *strong mass segregation*, is obtained with density scaling as $\rho_H(r)\sim r^{-\alpha}$, where $\alpha \gtrsim 2$. They have shown that there are two branches for the solution parameterized by $\Delta = \frac{N_H M_H^2}{N_L M_L^2}\cdot\frac{4}{3+M_H/M_L}$. The *weak* branch, for $\Delta > 1$, corresponds to the scaling relations found by BW77; while the *strong* branch, for $\Delta < 1$, generalizes the BW77 solution. There is a straightforward physical interpretation. In the limit where heavy stars are very scarce, they

barely interact with each other and instead sink to the center due to dynamical friction against the sea of light stars. Therefore, a quasi-steady state forms in which the heavy star's current is not nearly zero and thus the BW77 solution does not hold. As $\Delta$ increases, self-scattering of heavies becomes important and the resulting quasi-steady state forms with a nearly zero current for stars of all masses, so BW77 solution is recovered.

For all these reasons, it is fundamental to verify the Bahcall–Wolf solution—as well as its Alexander–Hopman generalization—with NB integrations. There has been a surprisingly small number of NB studies of multi-mass systems around an MBH (Baumgardt et al. 2004b; Freitag et al. 2006), and none of them reported the occurrence of strong mass segregation.

In this Letter, we use direct NB integrations to show for the first time that: (1) strong mass segregation is a robust outcome of the growth of stellar cusps around an MBH when $\Delta < 1$; (2) the BW77 solution is recovered when $\Delta > 1$; (3) as a corollary, we conclude that the rate of stellar ejections from the cusp is too low to destroy the high-density cusps around MBHs—even though ejections from the cusp *do* occur. Furthermore, having validated the FP formalism, we proceed to use it to estimate the timescales for cusp re-growth starting from a wider range of models. With our FP solutions we show that, for $M_\bullet \lesssim 5 \times 10^6\, M_\odot$, the times for re-growing stellar cusps are shorter than a Hubble time. Our results clearly suggest that strongly segregated stellar cusps around MBHs in this mass range may be quite common in NSCs and should be taken into account when estimating EMRI event rates.

## 2. MODELS AND INITIAL CONDITIONS

We have performed the NB simulations with a modified version of *NBODY4* (Aarseth 1999, 2003) adapted to the *GRAPE* − 6 special-purpose hardware. The code was modified to add the capture of stars by the MBH: stars that enter a critical radius $r_{\rm cap}$ from the hole are captured and their mass is added to the hole. The new position and velocity of the massive particle are calculated by imposing that capture processes conserve total linear momentum. The maximum number of particles in the memory of a micro-GRAPE board is $\sim 1.2 \times 10^5$, which has been shown to be sufficient to accurately describe the evolution of the bulk properties of the NSC (Preto et al. 2004), but is not enough to resolve its loss cone dynamics accurately. Therefore, we do not attempt a detailed modeling of tidal disruption processes and set the capture radius to be equal for all particles.

The MBH dominates the dynamics inside its influence radius $r_h$ defined to be the radius which encloses twice of its mass at $t = 0$. The stellar distribution evolves and reaches its asymptotic quasi-steady state over relaxation timescales (Spitzer 1987):

$$T_{rlx}(r_h) = 0.34 \frac{\sigma_h^3}{G^2 \rho_h m_* \ln \Lambda}, \qquad (1)$$

where $\sigma_h$ and $\rho_h$ are, respectively, the one-dimensional velocity dispersion and spatial density evaluated at $r_h$. Following Preto et al. (2004), we define the Coulomb logarithm $\ln \Lambda = \ln(r_h \sigma_h^2 / 2 G m_*)$, where $m_* = 1/N$.

A realistic mass population of stars with a continuous range of stellar masses can be approximately represented by two (well-separated) mass scales: one in the range $\mathcal{O}(1 M_\odot)$ corresponding to low-mass main-sequence stars, white dwarfs, and neutron stars; another with $\mathcal{O}(10 M_\odot)$ representing stellar black holes (SBHs). The relative abundance of objects in these mass ranges is overwhelmingly dominated by the lighter stars—typical number fractions of SBHs being $\mathcal{O}(10^{-3})$ (Alexander 2005).

**Table 1**
*N*-body Integrations

| Runs | $\gamma$ | $M_\bullet/M_g$ | $f_H$ | $\Delta$ | $r_h$ | $\ln \Lambda$ |
|---|---|---|---|---|---|---|
| 6 | 1 | 0.05 | $2.5 \times 10^{-3}$ | 0.08 | 0.46 | 8.3 |
| 6 | 1 | 0.05 | $5. \times 10^{-3}$ | 0.15 | 0.46 | 8.3 |
| 6 | 1 | 0.05 | $7.5 \times 10^{-3}$ | 0.23 | 0.46 | 8.3 |
| 6 | 1 | 0.05 | 0.01 | 0.31 | 0.46 | 8.3 |
| 4 | 1 | 0.05 | 0.429 | 13.2 | 0.46 | 8.3 |
| 2 | 1/2 | 0.01 | $2.5 \times 10^{-3}$ | 0.08 | 0.26 | 7.2 |
| 2 | 1/2 | 0.01 | $5. \times 10^{-3}$ | 0.15 | 0.26 | 7.2 |
| 2 | 1/2 | 0.01 | $7.5 \times 10^{-3}$ | 0.23 | 0.26 | 7.2 |
| 2 | 1/2 | 0.01 | 0.01 | 0.31 | 0.26 | 7.2 |

**Notes.** Column 1: number of runs; Column 2: slope of the Dehnen's model inner cusp at $t = 0$; Column 3: ratio of BH mass to total cluster mass in stars; Column 4: $f_H = N_H/N$ fraction of heavy mass particles; Column 5: Alexander & Hopman parameter; Column 6: influence radius $r_h$; Column 7: Coulomb logarithm at $r_h$. The total number of particles is $N = 1.24 \times 10^5$ in all runs; the mass ratio between heavy and light components is $R = 10$ for all runs. Tidal capture radius $r_{\rm cap} = 10^{-7}$ in all runs. We use units $G = M_{\rm nuc} = a = 1$, where $M_{\rm nuc}$ is the total mass of the nuclear cluster and $a$ is the Dehnen model's scale length.

The initial NSC is built from a Dehnen spherical model (Dehnen 1993) to which a massive particle is added at the center at rest (Tremaine et al. 1994). Positions and velocities are Monte Carlo realizations that accurately reproduce the spatial $\rho(r)$ and phase-space $f(E)$ densities with stars of the same mass. In order to generate a two-component model, we (1) specify the mass ratio $R = m_H/m_L$ between heavy and light stars, and respective number fractions $f_H = N_H/N$ and $f_L = 1 - f_H$, through which the AH09 $\Delta$ parameter is fixed and (2) assign the mass $m_H$ or $m_L$ randomly to each star according to the statistical weights $f_H$ and $f_L$, respectively. The resulting model is almost in dynamical equilibrium; deviations of virial ratio from unity are $\lesssim$1%–2%. On a dynamical timescale, phase mixing occurs, and the virial ratio converges to unity to within a fraction of a percent. Following this prescription, the two-component models start without any mass segregation, as would be expected from a violently relaxed system. Dehnen model's density has $\rho(r) \propto r^{-\gamma}$ at the center, and the corresponding distribution function $f(E)$ is isotropic. Table 1 gives the list of runs and adopted parameters.

## 3. FOKKER–PLANCK MODELS FOR SEVERAL STELLAR MASSES

We also study the evolution of NSCs with a multi-mass FP formalism and compare results with NB integrations. The time-dependent, orbit-averaged, isotropic, FP equation in energy space is defined, for each component (Spitzer 1987; Chernoff & Weinberg 1990), by

$$p(E) \frac{\partial f_i}{\partial t} = -\frac{\partial F_{E,i}}{\partial E}, \; F_{E,i} = -D_{EE,i} \frac{\partial f_i}{\partial E} - D_E f_i, \qquad (2)$$

$$D_{EE,i} = 4\pi^2 G^2 m_*^2 \mu_i^2 \ln \Lambda \times \sum_j^{N_c} \left[ \left( \frac{\mu_j}{\mu_i} \right)^2 q(E) \int_{-\infty}^{E} dE' f_j(E') + \int_E^{+\infty} dE' q(E') f_j(E') \right], \qquad (3)$$

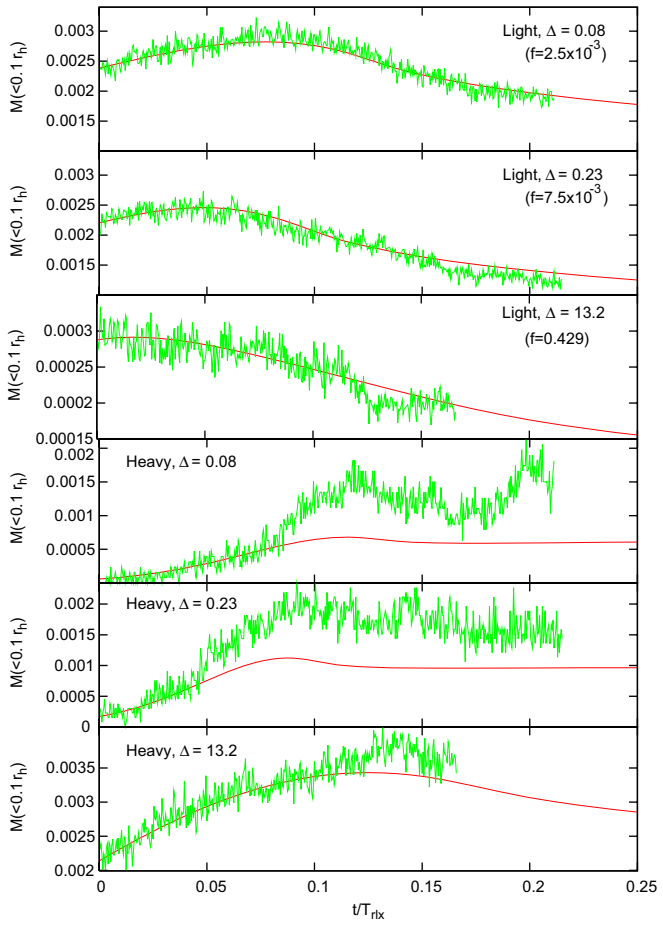


**Figure 1.** Evolution of stellar mass within 0.1 $r_h$ from the MBH, for light and heavy components. Smooth and noisy curves are from FP and NB integrations, respectively.

$$D_{E,i} = -\sum_{j}^{N_c}\left(\frac{\mu_j}{\mu_i}\right)\int_E^{+\infty} dE'\,p(E')f_j(E'). \qquad (4)$$

In this equation, $i$, $j$ run from 1 to $N_c$ (number of mass components), and $\mu_i = m_i/m_*$. $p(E) = 4\int_0^{r_{\max}(E)} dr\, r^2\sqrt{2(E-\Phi(r))}$ $= -\partial q/\partial E$ is the phase space accessible to each (bound) star of specific energy $E = -v^2/2 + \Phi(r) > 0$ (Spitzer 1987), and the total gravitational potential $\Phi(r)$ is the sum of the contribution from the nuclear cluster plus the hole. The stellar distribution and its resulting gravitational potential change substantially inside $r_h$ only, so we keep the contribution from the stars to total $\Phi(r)$ fixed throughout. This system of FP equations is more general than those from BW77 and AH09 in that it includes the dynamics of stars unbound to the MBH. It is also more general than those adopted by Merritt (2009) since it considers self-consistently two-body scattering between all components and it is, therefore, not limited to early evolution where the heavy component is just a small perturbation on the light component. As a result, we can follow both weak and strong branches of the solution throughout without restriction.

## 4. RESULTS

The density of stars around the MBH increases as the cusp grows for both light and heavy components until it reaches a quasi-steady state; afterward, the lights start to slowly expand. This can be seen in Figure 1, where the mass inside a sphere of $0.1r_h$, centered on the MBH, is depicted as a function of time. Curves from FP and NB are shown together for three different runs with $\Delta = 0.08, 0.23$ corresponding to strong segregation, and $\Delta = 13.2$ to weak segregation branches. Timescaling between NB and FP is related through $T_{rlx}^{\rm FP} = \ln\Lambda/N\ T_{rlx}^{\rm NB}$. In the three cases shown (as in all others cases tested but not shown), the agreement between both methods is very good, although there is a noticeable tendency for the heavy particles in the NB runs to segregate more strongly in the central cusp—this is especially the case in the strong branch. Figure 1 also suggests that a quasi-steady state (and maximum central concentration) have been reached by the end of the runs corresponding to $t \sim (0.1-0.2)T_{rlx}(r_h)$. We stress that mass segregation, whether in the weak or strong branch, speeds up cusp growth by factors ranging from 4 to 10 in comparison with the single-mass case (Preto et al. 2004). Figure 2 displays the spatial density profiles $\rho_L(r)$ and $\rho_H(r)$ at late times, $t \sim 0.2T_{rlx}(r_h)$. The agreement between both methods is again quite good although there is the tendency, in the strong branch, for NB's asymptotic slope $\gamma_L$ to be slightly smaller than in FP—for which $\gamma_{L,\rm min} = 1.5$. The slopes of the inner density profiles of the heavy component decrease as the solution evolves from the strong to the weak branch when $\Delta$ is increased, as expected. In the limit of $\Delta \gg 1$, $\gamma_H$ tends to evolve to a quasi-steady state close to the 7/4 solution, while for $\Delta \ll 1$, $\gamma_H \gtrsim 2$. The asymptotic inner

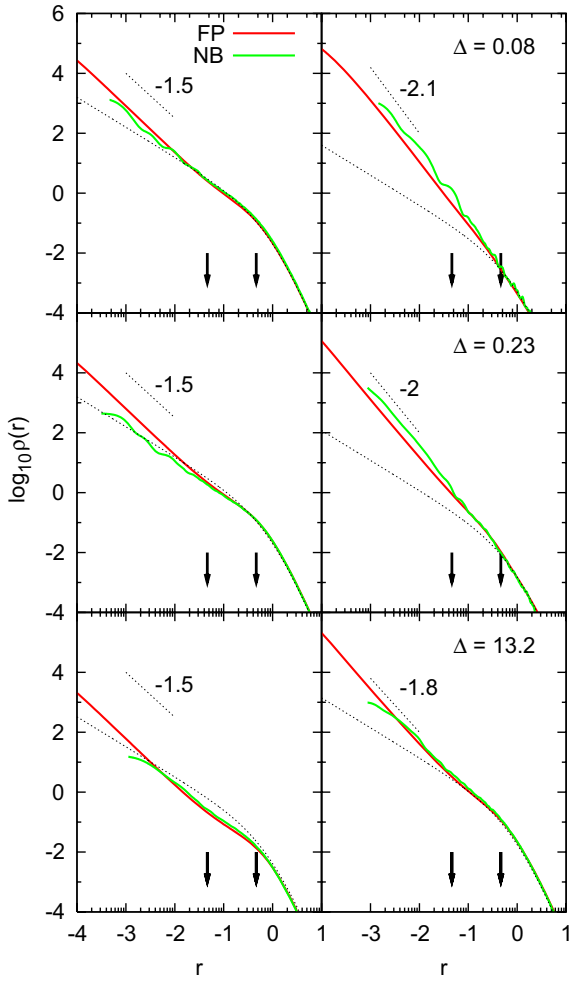


**Figure 2.** Mass density profiles, $\rho_L$(left) and $\rho_H$ (right), at the end of the integrations. Arrows signal location of $0.1r_h$ and $r_h$. The asymptotic slope $\gamma_H$ decreases from $\gtrsim 2$ to $\sim 7/4$ while moving from the strong to the weak branch of the solution.

density slopes, in both solution branches, of the light component extend out to $\sim 0.1 r_h$; in contrast, the heavy component shows a different behavior depending on the solution branch: on the weak branch, $\gamma_H$'s asymptotic slope also extends only up to $\sim 0.1 r_h$, while on the strong branch it extends virtually all the way to $r_h$. In the strong branch, the density of the heavy component exceeds that of the light for $r \lesssim 0.01 r_h$ (and will therefore dominate the interaction events with the MBH); in the weak branch, $\rho_H > \rho_L$ throughout.

Although there are some differences in quantitative detail, these NB results broadly confirm the FP calculations and validate its inherent assumptions—at least in what concerns the description of the *bulk* properties of stellar distributions.

## 5. IMPLICATION FOR GALACTIC NUCLEI AND SOURCES OF GWs

Analysis of the number counts of spectroscopically identified old stars in the sub-parsec region of our own Milky Way (Buchholz et al. 2009; Do et al. 2009)—believed to be complete down to magnitude $K = 15.5$—reveals a deficit of old stars with respect to the high number a strongly segregated cusp would entail. Although the slope of the density profile is still weakly constrained, the best fits from number counts data seem to exclude with certainty slopes $\gamma > 1$ (Schödel et al. 2009), and there could be a core with a stellar density decreasing toward the center, $\gamma < 0$, although such a fit is only marginally better than one with $\gamma \sim 1/2$.

Although we deem it to be too early to conclude the inexistence of a segregated cusp around Sgr$A^*$, since the detectable stars (essentially giants) are still a small fraction of the stellar population as a whole, we next compute the time necessary for cusp growth if at some point a central core is carved in the stellar distribution. Having validated the FP approach and its results, we study Equations (2) and (3), which are orders of magnitude faster to solve than NB integrations.

We choose as an initial condition a model with $\gamma = 1/2$, since the isotropization time—the time necessary for the establishment of this shallow cusp starting from a hole in the spatial distribution—is $\ll T_{rlx}(r_h)$ (Merritt 2009), and we are interested in the evolution over $O(T_{rlx})$ timescales. Figure 3 shows the evolving phase-space $f(E)$ and spatial $\rho(r)$ densities for both components ($R = 10$ and $f_H = 0.001$ constitute our fiducial case). It can be seen that, by $t \sim 0.25\ T_{rlx}(r_h)$, cusps with $\gamma_L \sim 1.5$ and $\gamma_H \sim 2$ (or $p_L \sim 0.05$ and $p_H \sim 0.5$ in phase space) are fully developed; a little earlier, at $t \sim 0.2\ T_{rlx}(r_h)$, the density cusp $\rho_H(r)$ is already fully developed down to $r \sim 0.01 r_h$ ($\sim 0.02$ pc if scaled to the Milky Way nucleus).

In order to convert our timescales to years in the Milky Way nucleus: (1) we adopt $M_\bullet = 0.05\, M_{\rm nuc}$, meaning the nucleus weighs $8 \times 10^7\ M_\odot$; (2) the radius enclosing $10^6\ M_\odot$ is 1 pc; and (3) using Equation (1), we obtain $T_{rlx}(2.5\ {\rm pc}) \sim 24$ Gyr consistent with Merritt (2009). If there was some event carving a hole in the stellar distribution around Sgr$A^*$ more than 6 Gyr ago, then there was enough time for a very steep cusp of SBHs to have re-grown. Merritt (2009) overestimated the time for cusp re-growth by neglecting heavy–heavy and heavy–light scattering. This is only approximately valid as long as $\rho_H \ll \rho_L$. The comparison of our Figure 3 with Figure 14 from Merritt (2009) shows that early evolution is similar, but after $\sim 2$ Gyr our full FP solution starts to evolve faster. This corresponds exactly to when the assumption $\rho_H \ll \rho_L$ is no longer valid.

The number fraction $f_H$ of SBHs is sensitive to the initial mass function (IMF) of high-mass stars. There are indications the IMF in galactic nuclei is top heavy (Maness et al. 2007) so we adopt a range of values $f_H \in [10^{-3}, 10^{-2}]$; the mass distribution of SBHs is also weakly constrained so we follow O'Leary et al. (2009) in considering several mass ratios $R = 10, 15$, and 20. Figure 4 shows the relaxation times at the influence radius for nuclei with MBH masses in the range of interest for *LISA*; the straight line is a linear fit to the points. The shaded region corresponds to the range $[0.1\ T_{rlx}(r_h), 0.2\ T_{rlx}(r_h)]$ and represents the time stellar cusps take to grow starting from an isotropic core. The shaded region's width results from the distribution of values for $R$ and $f$. In the ranges we adopted, increasing $R$ or $f_H$ both has the effect of decreasing the time for cusp growth. At early times, SBHs essentially evolve under dynamical friction with characteristic timescale $T_{df} \sim T_{rlx}/R$; increasing $f_H$ leads to an increased rate of self-scattering between SBHs at late times.

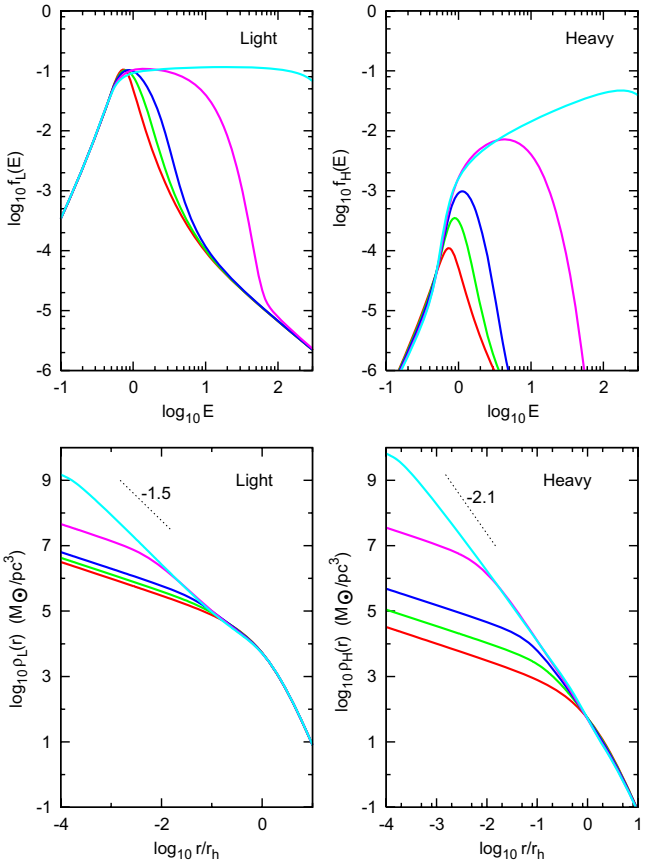


**Figure 3.** Phase-space and spatial densities (upper and lower panels, respectively). Model starts with $\gamma = 1/2$; $f_H = 10^{-3}$ and $R = 10$. Densities increase monotonically with time and are plotted at $t/T_{rlx} = 0, 0.05, 0.1, 0.2, 0.25$.

## 6. SUMMARY AND DISCUSSION

Our results show that strong mass segregation is a *robust* outcome from the growth of stellar cusps around MBHs. We have used NB integrations with two masses—light and heavy components representing main-sequence stars and SBHs respectively—and compared the results with those obtained with the FP formalism. The broad agreement between both methods validates the FP description of the *bulk* properties of time-evolving stellar distribution around a MBH—and its underlying assumptions.

Using the FP equation to study cusp growth under a variety of initial conditions purported to represent cored nuclei, we have

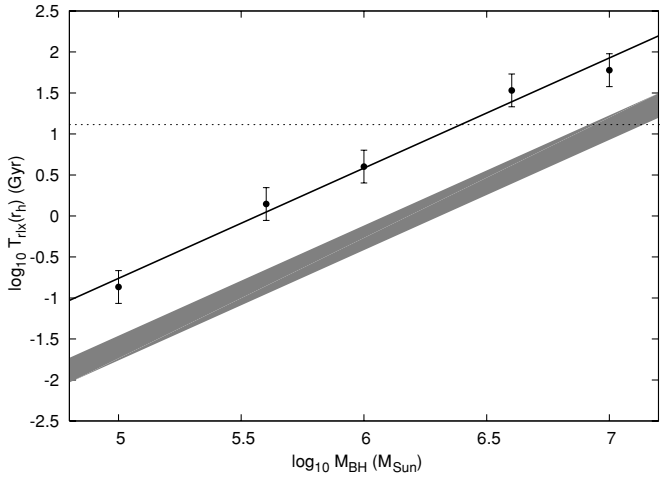


**Figure 4.** Single-mass relaxation time at $r_h$ for single-mass, cored models as a function of MBH mass. The shaded area covers $[0.1T_{rlx}, 0.2T_{rlx}]$—the time for cusp re-growth. Its finite width results from the distribution of parameters. The horizontal curve signals 13 Gyr.

shown that the timescales associated with cusp re-growth are clearly shorter than a Hubble time for nuclei with MBHs in the mass range $M_\bullet \lesssim 5 \times 10^6 M_\odot$—even though the relaxation time, as estimated for a single-mass stellar distribution, exceeds a Hubble time in the upper part of this mass range. Therefore, our work strongly suggests that quasi-steady—strongly segregated—stellar cusps may be common around MBHs with masses in this range.

EMRIs of compact remnants will be detectable by *LISA* precisely for MBHs in this mass range (de Freitas Pacheco et al. 2006; Amaro-Seoane et al. 2007; Babak et al. 2007). Estimates for event and detection rates by *LISA* customarily assume that the stellar cusps are in steady state (Hopman & Alexander 2006a, 2006b). But recent observations reveal a dearth of giants inside 1 pc from Sgr$A^*$ and raise the possibility that cored nuclei are common—this scenario has been thoroughly explored by Merritt (2009).

Although stellar cusps may re-grow in less than a Hubble time, the existence of cored nuclei still remains plausible—especially for nuclei with MBHs in the upper part of the mass range—since re-growth timescales are still quite long (e.g., 6 Gyr in Milky Way type nuclei). However, since EMRI detection rates by *LISA* are expected to peak around $M_\bullet \sim 4 \times 10^5$–$10^6\, M_\odot$ (Gair 2009), and re-growth times are $\lesssim$1 Gyr for $M_\bullet \lesssim 1.2 \times 10^6 M_\odot$, we still expect that a substantial fraction of EMRI events will originate from segregated stellar cusps. Finally, indirect observations alone will reveal whether there is a "hidden" cusp of old stars and their dark remnants around Sgr$A^*$ (Weinberg et al. 2005; Preto & Saha 2009).

M.P. and P.A.S. acknowledge support by Deutsches Zentrum für Luft- und Raumfahrt (DLR). The simulations have been carried out on the dedicated high-performance GRAPE-6A clusters at the Astronomisches Rechen-Institut in Heidelberg[4] and the Tuffstein cluster of the AEI.

## REFERENCES

Aarseth, S. J. 1999, PASP, 111, 1333
Aarseth, S. J. 2003, Gravitational N-Body Simulations (Cambridge: Cambridge Univ. Press)
Alexander, T. 2005, Phys. Rep., 419, 65
Alexander, T., & Hopman, C. 2009, ApJ, 697, 1861
Amaro-Seoane, P., Gair, J. R., Freitag, M., Miller, M. C., Mandel, I., Cutler, C. J., & Babak, S. 2007, Class. Quantum Grav., 17, 113
Babak, S., Fang, H., Gair, J. R., Glampedakis, K., & Hughes, S. A. 2007, Phys. Rev. D, 75, 024005
Bahcall, J., & Wolf, R. 1976, ApJ, 209, 214
Bahcall, J., & Wolf, R. 1977, ApJ, 216, 883
Baumgardt, H., Makino, J., & Ebisuzaki, T. 2004a, ApJ, 613, 1133
Baumgardt, H., Makino, J., & Ebisuzaki, T. 2004b, ApJ, 613, 1143
Buchholz, R., Schödel, R., & Eckart, A. 2009, A&A, 499, 483
Chernoff, D. F., & Weinberg, M. D. 1990, ApJ, 351, 121
Dehnen, W. 1993, MNRAS, 265, 250
de Freitas Pacheco, J. A., Filloux, C., & Regimbau, T. 2006, Phys. Rev. D, 74, 023001
Do, T., Ghez, A. M., Morris, M. R., Lu, J. R., Matthews, K., Yelda, S., & Larkin, J. 2009, ApJ, 703, 1323
Freitag, M., Amaro-Seoane, P., & Kalogera, V. 2006, ApJ, 649, 91
Gair, J. 2009, Class. Quantum Grav., 26, 094034
Graham, A. W., & Spitler, L. R. 2009, MNRAS, 397, 2148
Hénon, M. 1969, A&A, 2, 151
Hopman, C., & Alexander, T. 2005, ApJ, 629, 362
Hopman, C., & Alexander, T. 2006a, ApJ, 645, 1152
Hopman, C., & Alexander, T. 2006b, ApJ, 645, 133
Khalisi, E., Amaro-Seoane, P., & Spurzem, R. 2007, MNRAS, 374, 703
Lightman, A. P., & Shapiro, S. L. 1977, ApJ, 211, 244
Maness, H., et al. 2007, ApJ, 669, 1024
Merritt, D. 2009, arXiv:0909.1318
O'Leary, R., Kocsis, B., & Loeb, A. 2009, MNRAS, 395, 2127
Preto, M., Merritt, D., & Spurzem, R. 2004, ApJ, 613, L109
Preto, M., & Saha, P. 2009, ApJ, 703, 1743
Schödel, R., Merritt, D., & Eckart, A. 2009, A&A, 502, 91
Spitzer, L. 1987, Dynamical Evolution of Globular Clusters (Princeton, NJ: Princeton Univ. Press), 191
Tremaine, S., Richstone, D. O., Byun, Y.-I., Dressler, A., Faber, S. M., Grillmair, C., Kormendy, J., & Lauer, T. R. 1994, AJ, 107, 634
Weinberg, N. N., Milosavljević, M., & Ghez, A. M. 2005, ApJ, 622, 878

[4] GRACE: see http://www.ari.uni-heidelberg.de/grace